Toxicology Mechanisms and Methods

ISSN: (Print) (Online) Journal homepage: https://www.tandfonline.com/loi/itxm20

# New Multi-Walled carbon nanotube of industrial interest induce cell death in murine fibroblast cells

Krissia Franco de Godoy, Joice Margareth de Almeida Rodolpho, Patricia Brassolatti, Bruna Dias de Lima Fragelli, Cynthia Aparecida de Castro, Marcelo Assis, Juliana Cancino Bernardi, Ricardo de Oliveira Correia, Yulli Roxenne Albuquerque, Carlos Speglich, Elson Longo & Fernanda de Freitas Anibal

**To cite this article:** Krissia Franco de Godoy, Joice Margareth de Almeida Rodolpho, Patricia Brassolatti, Bruna Dias de Lima Fragelli, Cynthia Aparecida de Castro, Marcelo Assis, Juliana Cancino Bernardi, Ricardo de Oliveira Correia, Yulli Roxenne Albuquerque, Carlos Speglich, Elson Longo & Fernanda de Freitas Anibal (2021) New Multi-Walled carbon nanotube of industrial interest induce cell death in murine fibroblast cells, Toxicology Mechanisms and Methods, 31:7, 517-530, DOI: 10.1080/15376516.2021.1930311

**To link to this article:** https://doi.org/10.1080/15376516.2021.1930311

TOXICOLOGY MECHANISMS AND METHODS
2021, VOL. 31, NO. 7, 517–530
https://doi.org/10.1080/15376516.2021.1930311

Taylor & Francis
Taylor & Francis Group

RESEARCH ARTICLE



# New Multi-Walled carbon nanotube of industrial interest induce cell death in murine fibroblast cells

Krissia Franco de Godoy[a], Joice Margareth de Almeida Rodolpho[a], Patricia Brassolatti[a], Bruna Dias de Lima Fragelli[a], Cynthia Aparecida de Castro[a], Marcelo Assis[b], Juliana Cancino Bernardi[c], Ricardo de Oliveira Correia[a], Yulli Roxenne Albuquerque[a], Carlos Speglich[d], Elson Longo[b] and Fernanda de Freitas Anibal[a]

[a]Departamento de Morfologia e Patologia, Laboratório de Inflamação e Doenças Infecciosas, Universidade Federal de São Carlos, São Carlos, Brazil; [b]Departamento de Química, Centro de Desenvolvimento de Materiais Funcionais, Universidade Federal de São Carlos, São Carlos, Brazil; [c]Grupo de Nanomedicina e Nanotoxicologia, Instituto de Física de São Carlos, Universidade de São Paulo, São Carlos, São Paulo, Brazil; [d]Centro de Pesquisa Leopoldo Américo Miguez de Mello CENPES/Petróbras, Rio de Janeiro, RJ, Brazil

**ABSTRACT**

The search for new nanomaterials has brought to the multifactorial industry several opportunities for use and applications for existing materials. Carbon nanotubes (CNT), for example, present excellent properties which allow us to assume a series of applications, however there is concern in the industrial scope about possible adverse health effects related to constant exposure for inhalation or direct skin contact. Thus, using cell models is the fastest and safest way to assess the effects of a new material. The aim of this study was to investigate the cytotoxic profile in LA9 murine fibroblast lineage, of a new multi-walled carbon nanotube (MWCNT) that was functionalized with tetraethylenepentamine (TEPA) to obtain better physical-chemical characteristics for industrial use. The modifications presented in the CNT cause concern, as they can change its initial characteristics, making this nanomaterial harmful. HR-TEM, FE-SEM and zeta potential were used for the characterization. Cytotoxicity and cell proliferation tests, oxidative and nitrosative stress analyzes and inflammatory cytokine assay (TNF-α) were performed. The main findings demonstrated a reduction in cell viability, increased release of intracellular ROS, accompanied by an increase in TNF-α, indicating an important inflammatory profile. Confirmation of the data was performed by flow cytometry and ImageXpress with apoptosis/necrosis markers. These data provide initial evidence that OCNT-TEPA has a cytotoxic profile dependent on the concentration of LA9 fibroblasts, since there was an increase in free radicals, inflammation induction and cell death, suggesting that continuous exposure to this nanoparticle can cause damage to different tissues in the organism.

**ARTICLE HISTORY**
Received 22 January 2021
Revised 22 March 2021
Accepted 10 May 2021

**KEYWORDS**
Nanomaterials; nanoparticles; multi-walled carbon nanotube; cytotoxicity; inflammation; apoptosis/necrosis; murine fibroblast cells

## Introduction

Nanotechnology is one of the most promising areas of the 21st century for developing diverse types of materials made on a nanoscale (1–100 nm). Currently, the applications coming from this area in the most varied industrial sectors, attract investments that exceed millions of dollars per year worldwide, and as a result of the growing diversity of nanoproducts, an evaluation of its impacts on human beings and the environment is crucial (Nel et al. 2006; Savolainen et al. 2010).

The economic and scientific value generated by studies and applications of nanoparticles (NPs) can increase risks to living beings and the environment, reaching aquatic and terrestrial ecosystems (Patil and Lekhak 2020). The impact on the environment is highlighted by the large manufacturers and laboratories that synthesize and study these NPs, as they are considered as the main sources of product release (Bicho et al. 2020; Pikula, Chaika, et al. 2020; Zhao et al. 2020)

Studies describe that NPs may be present in the aquatic environment by means of surface washing, atmospheric sedimentation and direct spills that occur during their synthesis, application and use, causing the biochemical composition of microalgae to be compromised and interfering in the levels of the food chain. (Pikula, Chaika, et al. 2020). This generates an important field in science that would be to evaluate the interaction of NPs in biological organisms to obtain safe standards in the production and use of these nanomaterials, mimicking the problems faced by nanotechnology and nanotoxicology (Jeevanandam et al. 2018; Pikula, Chaika, et al. 2020; Pikula, Zakharenko, et al. 2020).

Among the different types of NPs, carbon compounds stand out for being a versatile element throughout the universe and, according to their arrangement of atoms, different

CONTACT Krissia Franco de Godoy krissia.fgodoy@gmail.com; Fernanda de Freitas Anibal ffanibal@ufscar.br Rod. Washington Luís, Km 235 Caixa Postal 676, CEP. 13565-905, São Carlos, SP, Brazil

Supplemental data for this article can be accessed here.

properties and formulations can be developed, such as black nanoparticles, diamond, graphite, fullerenes, carbon nanotubes (CNTs), carbon foams, graphene, carbon spots, fibers, among others (Hurt et al. 2006; Du et al. 2011; Aqel et al. 2012; Georgakilas et al. 2015; Veloz-Castillo et al. 2020)

Carbon nanotubes (CNTs) can be classified into two main forms that will differ in structure, length and number of layers: single-walled CNTs (SWCNTs) and multiple-walled CNTs (MWCNTs) (DI Cristo et al. 2019; Mohanta et al. 2019).

Since their discovery, MWCNT have attracted much interest due to their excellent physical-active, electrical and mechanical properties, also being increasingly used in a wide range of applications, such as microelectronics, energy storage, biosensors, oil wells and biomedicine (Endo 1988; Iijima 1991; Michael et al. 2013; Prajapati et al. 2020). However, despite having potential in applications in modern science and technology (Yuan 2019), some characteristics of their fibers, such as extreme aspect ratio, low specific density, and low solubility are worrisome, since that can trigger undesirable cytotoxic reactions, as observed for example, in asbestos fibers (Kobayashi et al. 2017).

In turn, cytotoxicity is related to the interaction of CNTs in the cellular environment, which in this case occurs in different ways (endocytosis, phagocytosis or needle-shaped penetration), which can trigger changes in cell cycle signaling and regulation (Aschberger et al. 2010; Firme and Bandaru 2010). The penetration of CNTs through the cell lipid bilayer membrane induces oxidative stress, free radical production, damage to proteins, impairment of genetic material and inflammation (Clichici et al. 2012; Mohanta et al. 2019; Prajapati et al. 2020). In addition, from a physicochemical point of view, this cytotoxicity is directly influenced by the type of nanoparticle, size, composition, surface charge, morphology, porosity, aggregation and solubility (Holsapple et al. 2005; Khan et al. 2019).

The current literature points to some of these toxic characteristics triggered by MWCNTs in different cell (fibroblasts, macrophages, keratinocytes, and lung cells) in *in vitro* models (Mannerström et al. 2016; Binelli et al. 2018). However, the diversity in the investigated protocols must be taken into account, such as differences between the type of carbon, sizes and morpho functional characteristics, concentration used and also the type of cells evaluated. As a result, it becomes imperative to highlight the difficulty in comparing the results found and to clearly demonstrate its effects on human beings and the environment. Therefore, it is considered that the use of CNTs in the industrial scope and the concern related to biosafety increase linearly (DI Cristo et al. 2019; Yuan 2019), and that is why it is essential to make a careful assessment of the main aspects and possible cellular interactions of a newly synthesized nanoparticle, for later inclusion of its market use (Yoksan and Chirachanchai 2008; Beer et al. 2012; Jain et al. 2012; Torresan and Wolosiuk 2021).

In the present study, a new carbon nanoparticle of industrial interest, called OCNT-TEPA, will be used, synthesized from a MWCNT oxidized to OCNT and subjected to the insertion of a tetraethylenepentamine (TEPA) ligand on its surface, giving rise to OCNT – TEPA. The insertion of this binder had the intuition to improve some characteristics of the nanoparticle for its application, generating a nanofluid with greater thermal stability, better viscosity, resistant to high temperatures and salinity, since nanofluids are widely used in the oil and gas industry (Lima et al. 2018). However, the consequences caused by the modification with the TEPA polymer is of great concern because this functionalization of the CNT can alter conformation, surface area and physic-chemical properties, making OCNT-TEPA a nanoparticle with the potential to trigger undesirable toxicity mechanisms. Therefore, this study presents an exclusive evaluation of the OCNT-TEPA cytotoxic profile in the LA9 murine fibroblast lineage with acute exposure phase, to identify possible damage through the oxidative and inflammatory profile, in addition to determining which metabolic pathways are involved in this process.

## Materials and methods

### *Nanoparticle*

The OCNT-TEPA carbon nanoparticle was provided by the petroleum industry PETROBRAS.

### *Characterization and potential zeta of OCNT-TEPA*

The OCNT-TEPA samples were analyzed by field emission scanning electron microscope (FE-SEM), using a Supra 35-VP (Carl Zeiss) operated at 2 kV. The samples were washed with water three times to remove organic residues, dripped onto a Si plate and dried at 60 °C. A high-resolution transmission electron microscope Jem-2100 LaB6 (Jeol) (HR-TEM) with a voltage of 200 kV acceleration coupled to an INCA Energy TEM 200 (Oxford) was used to obtain larger magnifications and to clearly verify the MWCNT samples. The samples were prepared by ultrasonic dispersion of the MWCNTs samples in water depositing small amounts in Cu grades coated with drilled C.

The zeta potential of the OCNT-TEPA) was evaluated using a Malvern spectrometer Nano-ZS (Marvern Instruments). The results are presented as mean ± SD resulting from three different measurements.

The experimental design is inserted in the Supplementary Figure 1.

### *Absorption and fluorescence spectroscopy*

The absorption spectroscopy measurements of the OCNT-TEPA samples were adjusted using the UV-Vis Cary 50 (Varian®) double-beam spectrophotometer with a 190–1100 nm spectrum, 1 cm plastic cuvettes and coupled to a microcomputer. Detection was made from 400 to 800 nm. The photoluminescent behavior of OCNT-TEPA was evaluated by fluorescence spectroscopy. Measurements were performed on a Cary Eclipse Spectrofluorometer (Fluorescence Spectrophotometer – Agilent Technologies), using a 96-well white plate to reduce cross interference in luminescent

assays. The acquisitions were made by stimulating the samples at 450 nm and collecting data from 470 to 800 nm.

### Cell culture

The fibroblast cell line LA9 (code 0142) from mouse adipose tissue obtained from the Rio de Janeiro cell bank (BCRJ), was grown in Dulbecco's Modified Eagle's Medium (DMEM) (Sigma-Aldrich, USA) supplemented with 10% fetal bovine serum (FBS) (LGC Biotechnology) and incubated at 37 °C and 5% $CO_2$. The experimental protocol established was 3 independent experiments in and the concentrations of OCNT-TEPA tested were 1, 50, 250, 500, and 1000 μg/ml for 24 hours.

### Determination of concentrations of OCNT-TEPA, cytotoxicity assay with MTT and $EC_{50}$ determination

The cytotoxic activity of OCNT-TEPA was evaluated with the aid of the MTT colorimetric assay (MTT- [3- (4,5-dimethylthiazol-2-yl) 2,5-diphenyltetrazolium bromide] – Sigma-Aldrich, USA) that analyzes the integrity of mitochondrial function through the production of formazan crystals, proportionally, the lower the crystal production, the lower the cell viability (TIM Mosmann 1983). Initially the test was applied to determine which concentrations would be tested, based on the literature, which reported that the most studied concentrations for nanoparticles vary from 1 to 1000 μg/ml. The selection criterion was to use concentrations that proved to be more toxic and nontoxic among those initially tested (1, 10, 50, 100, 250, 500, 750 e 1000 μg/ml). The concentrations of 1, 50, 250, 500 and 1000 μg/ml were chosen to carry out the study. In a 96-well plate, $6 \times 03$ cells/well were seeded and exposed to OCNT-TEPA. After the exposure period, the wells were washed with PBS (phosphate buffered saline) 1X and the MTT solution (5 mg/ml) was added and the reaction occurred for 4 hours at 37 °C and 5% of $CO_2$. The formazan crystals formed were solubilized with 100 μl of DMSO and the absorbance was measured at 570 nm in a plate spectrophotometer (Thermo Scientific ™ Multiskan ™ GO Microplate Spectrophotometer). From the absorbance data, the EC50 (concentration that induces half the maximum effect) was calculated. The percentage of cytotoxicity occurred by comparing the data obtained with the Control group according to the equation below:

$$\%\ \text{cytotoxicity} = \frac{\text{Experimental group}}{\text{Control group mean}} \times 100$$

### LDH (lactate dehydrogenase)

Cytotoxicity damage to the cell membrane was measured according to the CyQuant ™ LDH Cytotoxicity Assay Kit (Invitrogen). In a 96-well plate, $1 \times 10^4$ cells/well were seeded and exposed to OCNT-TEPA for 24 hours. After the exposure period, the wells were washed with PBS 1X and the supernatant from each group was collected and 50 μL was added to a new plate. Then, 50 μL of the reagent solution was added to each well for 30 minutes in the absence of light and absorbance reading was measured at 490 nm and at 690 nm in a plate spectrophotometer (Thermo Scientific ™ Multiskan™ GO Microplate Spectrophotometer). To determine LDH activity, the values obtained at 680 nm from 490 nm were subtracted and the % cytotoxicity was calculated using the formula:

$$\%\ \text{cytotoxicity} = \frac{\textit{Experimental group} - \textit{spontaneous LDH activity}}{\textit{Maximum LDH activity} - \textit{spontaneous LDH activity}} \times 100$$

The wells of spontaneous LDH activity contained 10 μl of water and the maximum LDH activity contained 10 μl of lysis solution.

### Clonogenic assay

The evaluation of the capacity of a single cell to form colonies, which demonstrates the ability of cell recovery, after exposure to OCNT-TEPA occurred according to the adapted protocol of Franken et al (Franken et al. 2006). In a 6-well plate 1000 cells/well were seeded and exposed to OCNT–TEPA for 24 hours. Then, the wells were washed with PBS 1X and new DMEM was added. After 7 days, the cells were fixed with methanol and stained with 0.1% violet crystal. Each well was photographed and colonies were counted using the ImageJ 1.53a software. Plating efficiency was determined by dividing the number of colonies formed by the number of cells initially seeded. The survival fraction was determined by dividing the mean plating efficiency of cells exposed to OCNT-TEPA by the plating efficiency of the negative control. After cell counting, 1 ml of 1% SDS was added to the wells for colony solubility and possible quantification. The absorbance reading was measured at 570 nm in a plate spectrophotometer (Thermo Scientific ™ Multiskan ™ GO Microplate Spectrophotometer).

### Cell morphology by optical microscopy

The morphology of LA9 cells was observed after 24 hours of exposure to OCNT-TEPA using an optical microscope Axiovert 40 CFL (Zeiss), with a 10X objective lens, whose images were captured using the coupled camera model LOD-3000 (Bio Focus) and analyzed by the software Future WinJoeTM version 2.0 (Schindelin et al. 2012).

### Detection of reactive nitrogen species (RNS)

The production of nitric oxide was measured through the Griess reaction (Green et al. 1982; Saltzman 1954). In a 96-well plate, $1 \times 10^4$ cells/well were seeded and exposed to OCNT-TEPA for 24 hours. After the exposure time the supernatant from the wells was collected and 50 μl of the supernatant well pool was added in a 96-well plate and mixed with 50 μl of Griess reagent (1:1 mixture of solution A [1% sulfanilamide in acid phosphoric 5%] and solution B [0.1% N-1- naphthylethylenediamine dihydrochloride]), and

absorbance was measured at 540 nm in a plate spectrophotometer (Thermo Scientific ™ Multiskan ™ GO Microplate Spectrophotometer) after 15 minutes of reaction at room temperature. Sodium nitrite was used to construct the standard curve.

### Detection of reactive oxygen species (ROS)

The detection of the production of ROS was performed through the use of the fluorescent probe DCFH-DA (2′, 7′-Dichlorodihydrofluorescein Diacetate) (Sigma-Aldrich) (Wan et al. 1993). In a 96-well plate, $1 \times 10^4$ cells/well were seeded and exposed to OCNT-TEPA. After the exposure period, the medium was removed from the wells and the DCFH-DA probe solubilized in DMEM without FBS and without phenol was added to each well, the reaction took place for 30 minutes at 37 °C and 5% $CO_2$ protected from light. After that, the wells were washed with PBS 1X. The fluorescence emission reading was measured at 485-530 nm in a Spectra MAX i3 ® plate spectrophotometer (Molecular Devices). The percentage of cell viability was calculated using the same formula applied in the MTT test and described above.

Images of the LA9 cells were also produced with the DCFH-DA probe using the equipment ImageXpress® Micro XL Widefield High Content Screening System by Molecular Devices®) with a 20X objective lens.

### Quantification of TNF-α cytokines

The levels of cytokine TNF-α were measured using the ELISA quantification kit following the manufacturer's standards (BD Biosciences). In a 96-well plate, $1 \times 10^4$ cells/well were seeded and exposed to OCNT-TEPA for 24 hours. After the exposure period, the supernatant was collected and 50 µl of the pool of the supernatant well were added to a 96-well ELISA plate, already sensitized with capture antibody and blocked with milk proteins. Then, the secondary antibody conjugated with the peroxide enzyme was added and after 2 hours the enzymatic substrate (3,3′, 5,5′-Tetrametilbenzidina, TMB) was added to the wells revealing the reaction. The absorbance reading was measured at 450 nm in a plate spectrophotometer (Thermo Scientific ™ Multiskan™ GO Microplate Spectrophotometer) and the concentrations were calculated from a standard curve for each sample.

### Apoptosis – ImageXpress micro

The analyzes to determine cell death through images were performed using an automated high resolution epifluorescent microscopy system ImageXpress® Micro by Molecular Devices® equipment. In a 96-well plate, $1 \times 10^4$ cells/well were seeded and exposed to OCNT-TEPA for 24 hours. After the exposure time, the medium has been discarded and the wells were washed with PBS 1X. The plates were centrifuged centrifuged at 1500 g and at 4 °C and stained with an Acridine Orange (AO) and Propidium Iodide (PI) solution (Sigma-Aldrich) 1:1 ratio for 15 minutes at room temperature. Then, the wells were washed with PBS 1X and DMEM medium without FBS and without phenol was added. The images were obtained ImageXpress Micro with 40X objective lens and FITC and TexasRed filters with image overlay.

### Apoptosis – flow cytometry

The identification of cell death by apoptosis and necrosis occurred using the annexin V (PE and 7AAD) marker detection kit (BD Biosciences). In a 24-well plate, $1 \times 10^5$ cells/well were seeded and exposed for 24 hours to OCNT-TEPA. After the exposure period, the plates were centrifuged at 1500 g and at 4 °C and washed with PBS 1X and antibodies PE Anexin V and 7AAd [1: 1] (1 µl/well in 1:10 binding buffer) were added. The reaction lasted 15 minutes at room temperature protected from light. Then, the cells were removed with the aid of a scraper and resuspended in microtubes with 300 µl of binding buffer. Analyzes were performed on a flow cytometer (Accuri™ C6 BD Biosciences) with 10,000 events per gate using the software FlowJo™ version X (BD Biosciences).

### Statistical analysis

The results were analyzed using GraphPad Prism 7.0 (San Diego, California, USA) and Sigmaplot software (version 14). The identification of the discrepant data was performed through the Grubbs analysis, followed by the distribution of variables was tested using the normality (Shapiro-Wilk test) and equal variance (Levene method). For the analysis of multiple comparisons, one-way ANOVA with Tukey *post hoc* tests were used to evaluate the variance between groups for parametric data (results were presented in mean and standard deviation) and nonparametric data, the Kruskal–Wallis test was used with post hoc Dunn (results were presented as the median with the upper and lower quartiles: Me [Q1; Q3]). The statistical significance established is $p < 0.05$.

## Results

### Characterization of OCNT-TEPA

The Figure 1 shows the FE-SEM images at 100000X magnification. The Figure 1(a) shows OCNT-TEPA without contact with the culture medium, observing nanotubes with a low degree of agglomeration and an average diameter of 12.7 ± 3.0 nm. When OCNT-TEPA come into contact with the culture medium (Figure 1(b–f)), agglomerations of OCNT-TEPA are observed for all concentrations, being higher with the increase in the concentration of OCNT-TEPA. In addition, an increase in the average diameter of the OCNT-TEPA is observed, which decreases with the increase in the concentration of the OCNT-TEPA (27.3 ± 9.2, 20.6 ± 4.5, 18.0 ± 3.5, 17.4 ± 5.7 and 15.5 ± 4.8 for concentrations of 1, 50, 250, 500, and 1000 µg/ml). For the concentration of 1000 µg/ml of CNTs, there is still a compaction of OCNT-TEPA. To complement the FE-SEM images, HR-TEM images were performed to confirm the effects of agglomeration and densification of the

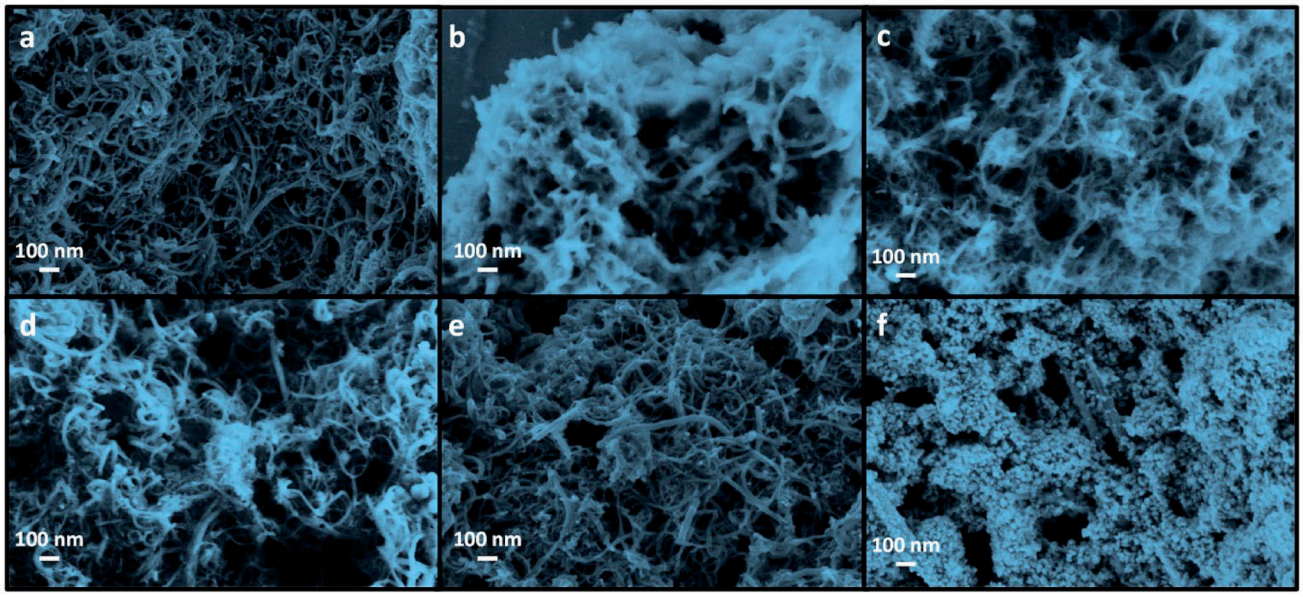


**Figure 1.** FE-SEM images at 100000× magnification for (a) pure OCNT-TEPA and at concentrations (b) 1, (c) 50, (d) 250, (e) 500 and (f) 1000 μg/ml.

samples due to interaction with the proteins of the culture medium and subsequent corona formation.

For OCNT-TEPA, a good dispersion is observed among the OCNT-TEPA samples (Figure 2(a)). In contrast, the aggregation factor is confirmed by the TEM images for concentrations of 500 and 1000 μg/ml (Figure 2(c,e)). In addition, dark regions of CNTs densification are observed for both concentrations, with greater emphasis on the concentration of 1000 μg/ml. These results are in line with those obtained by FE-SEM. For all samples, it is observed that the OCNT-TEPA found have more than one layer on their walls, characterizing them as multi walled (MWCNTs) (Figure 2(b,d,f)). The internal diameter of the OCNT-TEPA varies between 3.5 and 6.0 nm in all samples, and it is possible to observe the increase in the total diameter of the OCNT-TEPA when in contact with the culture medium.

The surface charge of OCNT-TEPA dispersed in different medium was compared by zeta potential measurements. The zeta potential of the suspension in water was approximately $-13.3 \pm 1.59$ mV, revealing a negative charged nanoparticle due to the prevalence presence of carboxyl groups at MWCNT surface even after TEPA modification. Zeta potential of OCNT-TEPA in culture medium further confirmed the decrease of their negative charge due to the corona protein formation as revealed by microscopies analyses. The zeta potential values indicated that charge has changed from less negative $-12.5 \pm 1.05$ mV in culture medium to $-9.21 \pm 1.24$ mV in culture medium + 10% FBS.

### *Absorption and fluorescence spectroscopy*

The absorption and fluorescence spectroscopy of OCNT-TEPA is shown in Figure 3. In absorption spectroscopy, the spectrometer casts a beam of light into the cuvette, collects the remaining light on the other side, so that we can see which wavelengths were absorbed or not at a given wavelength. This analysis then becomes important considering the objective of checking the fluorescence of OCNT-TEPA, since to understand the fluorescence spectrum it is also necessary to understand the absorption spectrum. In the absorption spectra we observed that the cuvette and the water remain as a baseline, but analyzing the OCNT-TEPA, we observed the scattering of the absorption light, with no peak or absorption bands in this range (400–800 nm) which is in agreement with this class of nanomaterial (Figure 3(a)) (Shetty et al. 2009; Yang et al. 2016). Analyzing the various concentrations of the OCNT-TEPA nanoparticle, we observed that the fluorescence curve pattern did not change compared with water. At higher concentrations the spectrum decreases their signal due to greater scattering of light that OCNT-TEPA can induce, decreasing the fluorescence emission signal (Figure 3(b)).

### *MTT assay and $EC_{50}$ determination*

The cytotoxicity in % of the different OCNT-TEPA nanoparticle concentrations in LA9 fibroblasts after 24 hours exposure made by the MTT assay is shown in Figure 4. A significant decrease in the values obtained related to cell viability was observed in the concentrations of 250, 500 and 1000 μg/ml of OCNT-TEPA when compared to the values obtained in the Control group, which represents a percentage of 45.04, 35.04 and 29.77%, respectively (Figure 4(a)). The $EC_{50}$ of the OCNT-TEPA nanoparticle was determined to be 115.5 μg/ml (Figure 4(b)) from the results obtained in the MTT assay.

### *LDH (lactate dehydrogenase)*

The cell viability shown from the measurement of LDH levels released from the OCNT-TEPA nanoparticle after 24 hours of exposure is shown in Figure 5. There was a significant increase in the values obtained in the group exposed to 1000 μg/ml when compared to the Control group, which represents a percentage of 18.79% (Figure 5(a)). Although there

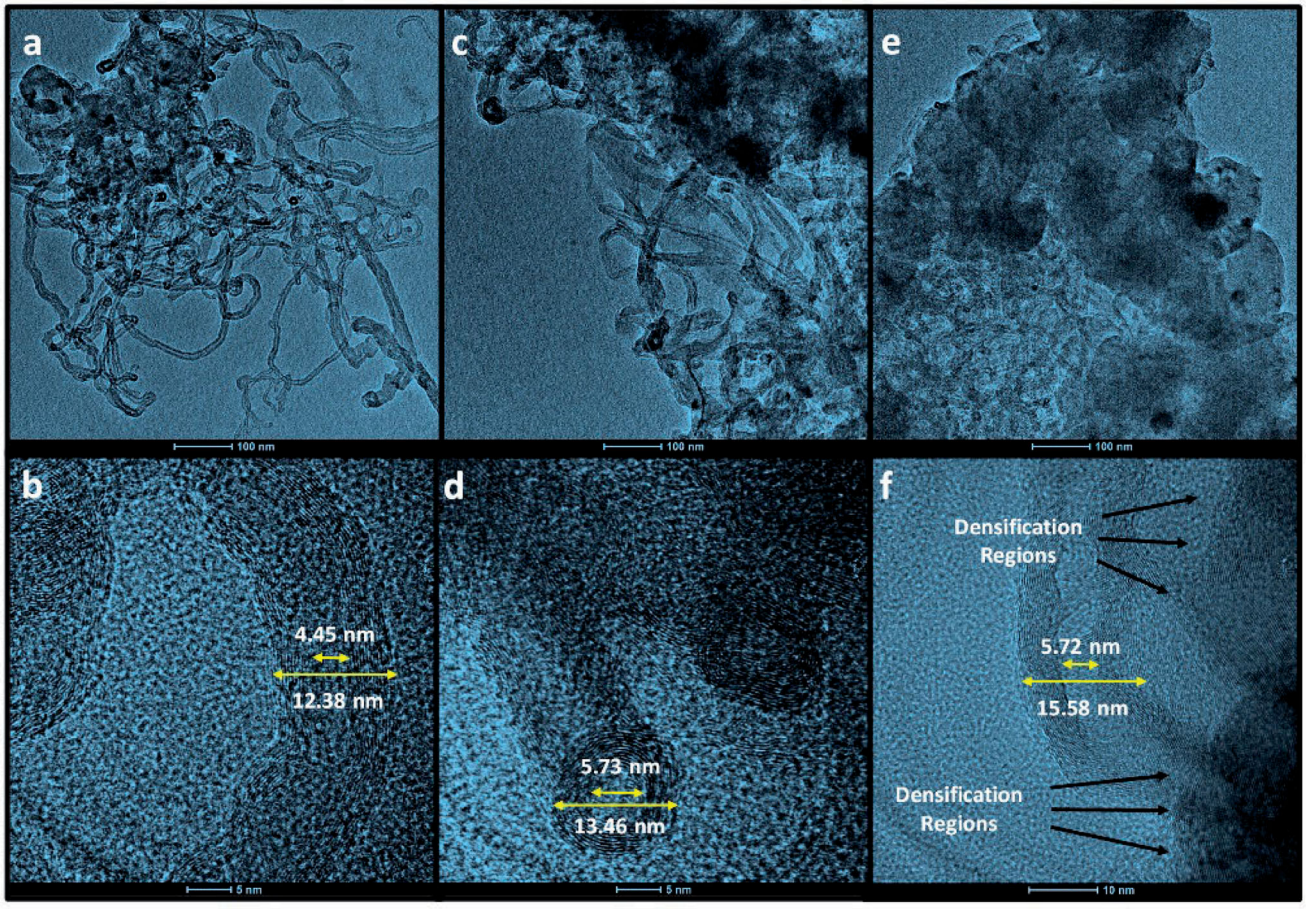


**Figure 2.** TEM and HR-TEM images for (a, b) pure OCNT-TEPA, and at concentrations (c, d) 500 and (e, f) 1000 μg/ml.

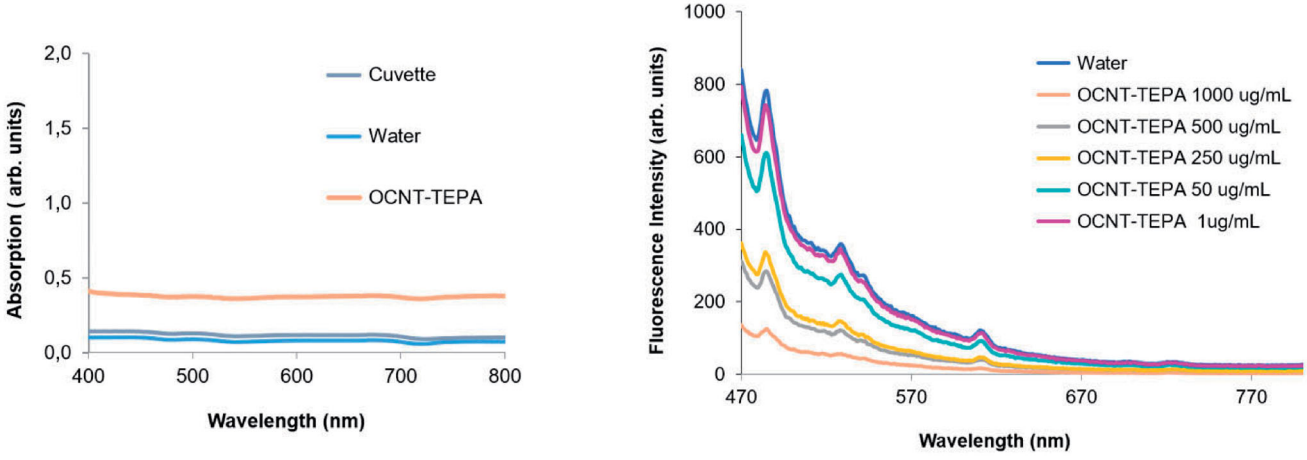


**Figure 3.** Spectroscopy of the OCNT-TEPA nanoparticle. (a) Spectral absorbance of OCNT-TEPA nanoparticle in water. (b) Autofluorescence (AF) emission spectrum of the OCNT-TEPA nanoparticle in different concentrations.

is no significant difference in the values of the other groups, it is possible to notice a slight increase in the LDH values released when analyzing the increase in concentrations.

The correlation between the MTT and LDH tests is because both complement each other, that is, the concentration that showed less mitochondrial activity was the same that increased the release of LDH, which is a membrane indicator disability (Figure 5(b)).

### *Clonogenic assay*

In the colony formation test (qualitative data), the results of the cell viability test (MTT and LDH) were confirmed and are shown in Figure 6. A significant decrease in the number of colonies was observed when exposed to concentrations of 250, 500, and 1000 μg/ml of OCNT-TEPA for 24 hours, compared to the control (Figure 6(a)). The Figure 6(b) reveals

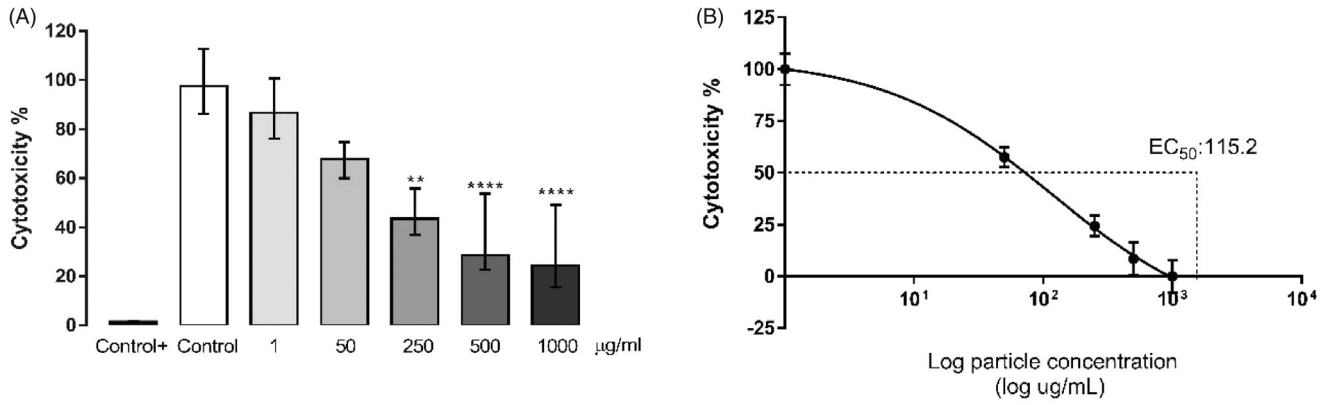


**Figure 4.** Concentration-response of cytotoxicity (%) in fibroblast LA-9 after 24 hours of exposure to different concentrations of OCNT-TEPA nanoparticle. Each analyzed concentration (1; 50; 250; 500 e 1000 µg/ml); Control+ (Extran 5%); Control (cells + medium). (a) Cell viability (%). (*) vs. Control; $*p < 0.5$; $**p < 0.01$; $***p < 0.001$; $****p < 0.0001$. (b) Demonstration of $EC_{50}$ values (curves). The results were presented as the median with the upper and lower quartiles: Me [Q1; Q3].

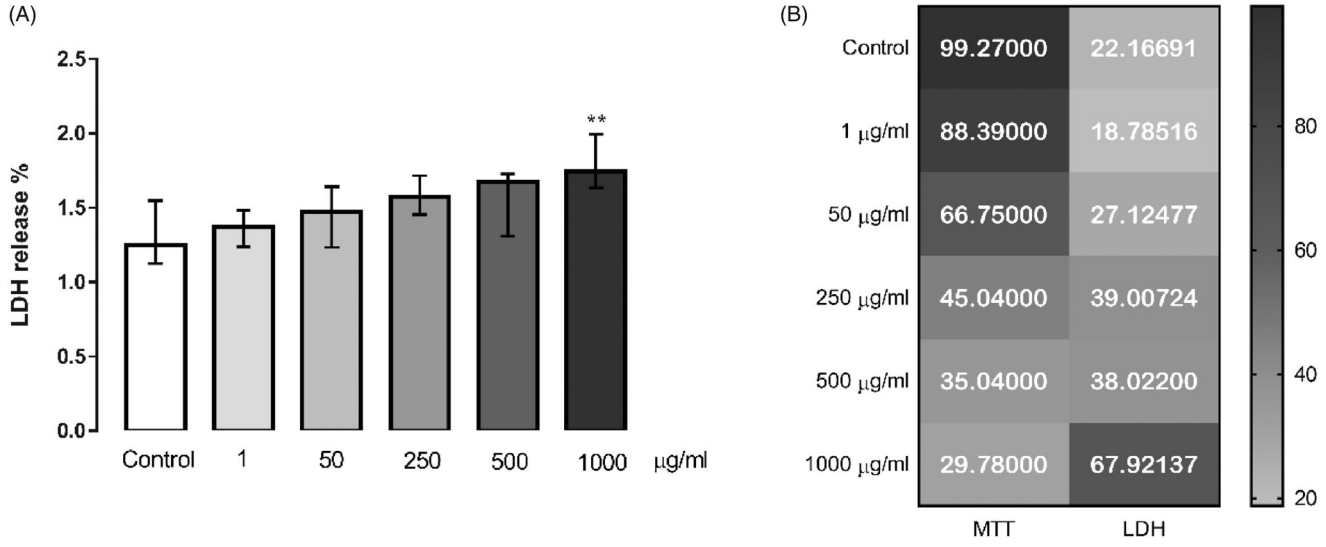


**Figure 5.** Response to cytotoxicity concentration (%) of fibroblasts LA-9 in 24 hours of exposure to OCNT-TEPA nanoparticle with LDH. Each analyzed concentration (1; 50; 250; 500 and 1000 µg/ml); Control (cells + medium). (a) Cell viability (%). (b) correlation between the MTT and LDH tests. (*) vs. Control; $*p < 0.5$ and $**p < 0.01$. The results were presented as the median with the upper and lower quartiles: Me [Q1; Q3].

that the concentrations of 250, 500, and 1000 µg/ml when quantified, by absorbance reading, after the colonies are detached from the plate, presented results similar to the image and the number of colonies (Figure 6(c)). As it is a non-colorimetric test, it allows us to certify all of our viability tests.

### *Cell morphology*

Cell morphology (qualitative data), was observed after 24 hours of exposure to different concentrations of OCNT-TEPA and is shown in Figure 7. The images demonstrated some changes in cell morphology when in contact with the highest concentrations of OCNT-TEPA, registering a smaller number of viable cells (250, 500, and 1000 µg/ml). When exposed to low concentrations of OCNT-TEPA, a greater number of cells is found, but with altered morphology compared to the control. These results corroborate the tests applied to cell viability, since in the highest concentrations we observed few whole intact cells, with probable cell lysis occurring.

### *Effect of functionalization density on RNS/ROS – Production reactive nitrogen species (RNS), reactive oxygen species (ROS) and immune responses*

The analysis to detect RNS in % was performed by measuring the production of nitric oxide (NO) by the Griess reaction in fibroblast cells LA9 exposed to different concentrations of OCNT-TEPA for 24 hours and is shown in Figure 8(a). There is a significant difference in the values obtained at concentrations of 500 and 1000 µg/ml of OCNT-TEPA when compared to the Control. The Figure 8(b) shows the ability of different concentrations of OCNT-TEPA to induce the formation of reactive intracellular oxygen species (ROS) in fibroblasts LA9 using DCF-DA fluorescence as an inducer of intracellular oxidant production. The exposure of the concentrations of 250, 500, and 1000 µg/ml of OCNT-TEPA generated significant difference in ROS production values in % when compared to

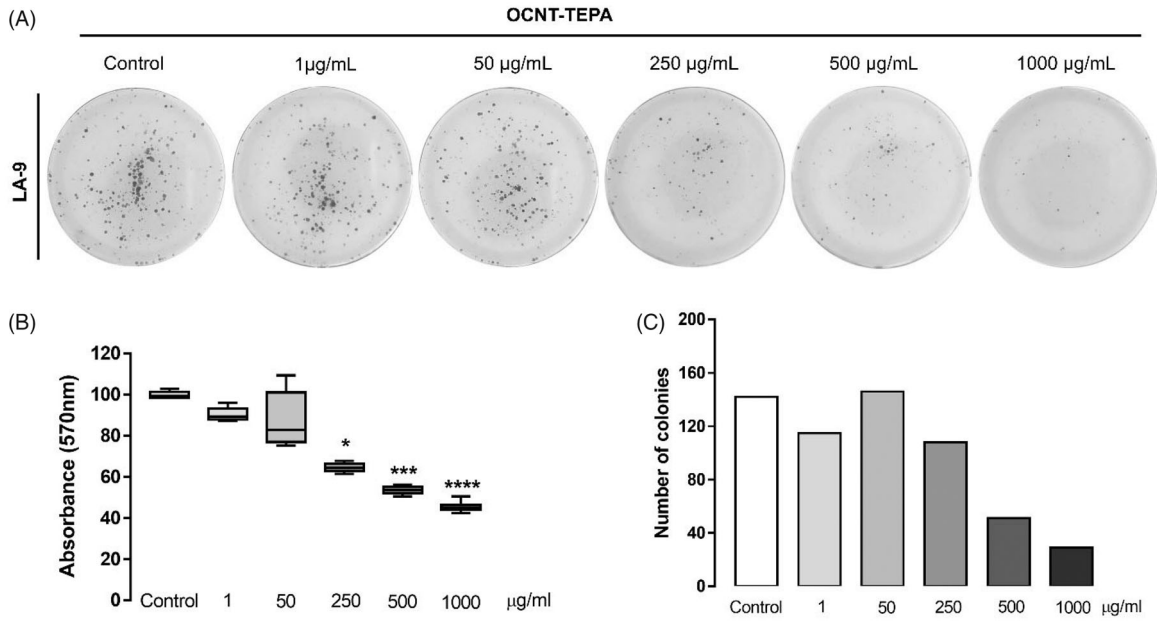


**Figure 6.** Effects of exposure to different concentrations of OCNT-TEPA on the formation of fibroblasts LA9 colonies after 24 hours. Each analyzed concentration (1; 50; 250; 500 and 1000 µg/ml); Control (cells + medium). (a) Colonies of fibroblasts cells after 7 days of recovery. (b) Quantification of absorbance of recovered colonies represented in percentage. (c) Number of colonies. (*) vs. Control; $*p < 0.5$ and $**p < 0.01$. The results were presented as the median with the upper and lower quartiles: Me [Q1; Q3].

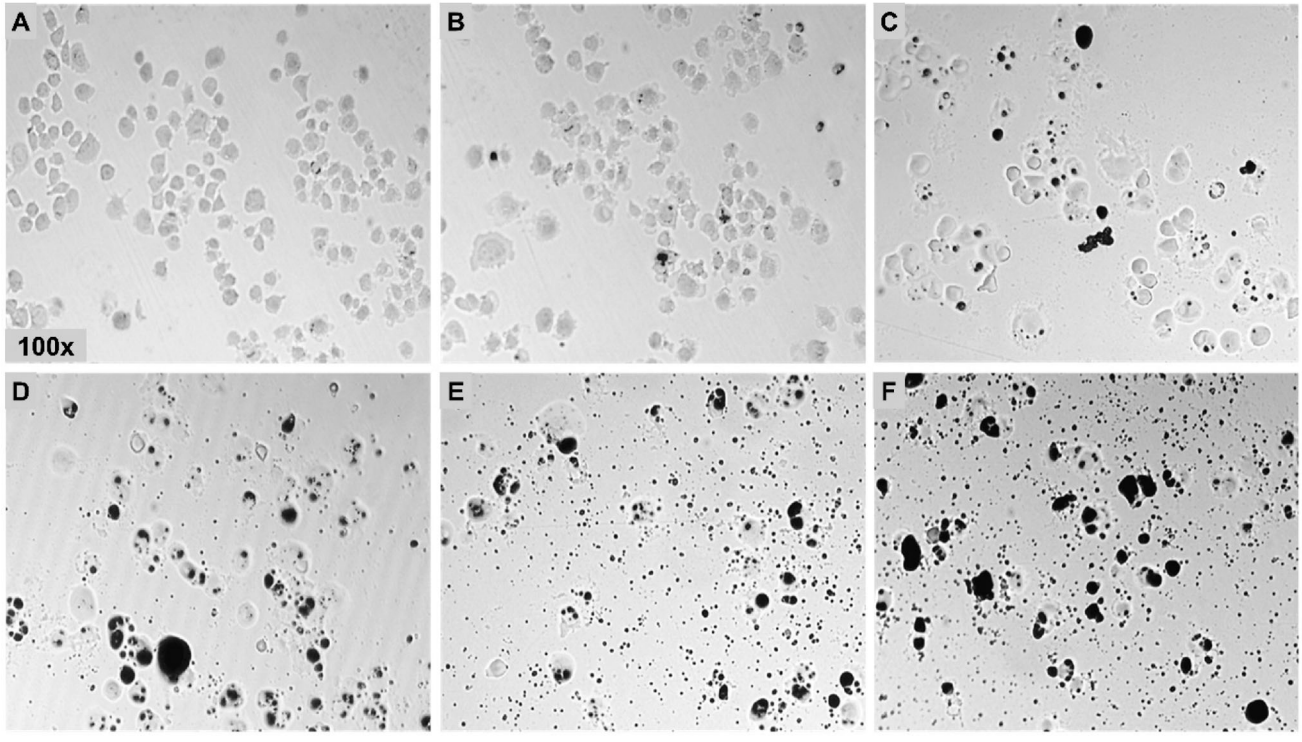


**Figure 7.** Cell morphology of fibroblast LA-9 24 hours of exposure to different concentrations of OCNT-TEPA: (a) control, (b) 1 µg/ml, (c) 50 µg/ml, (d) 250 µg/ml, (e) 500 µg/ml, and (f) 1000 µg/ml.

the Control. It was reported by means of images in Figure 8(d), the presence and intensity of production of ROS according to each concentration (qualitative data). It is worth mentioning that the production of ROS in the largest contractions of MWCNT ONCT-TEPA remained above the control levels (100%), that is, the production of ROS generated an approximate percentage of 1320, 1832, and 1884%, respectively, for the concentrations of 250, 500, and 1000 µg/ml.

The Figure 8(c) shows the dosage of the pro-inflammatory mediator TNF-α in response to 24-hour exposure to OCNT-TEPA in the fibroblast lineage LA9. TNF-α production was significantly observed at concentrations of 250, 500, and 1000 µg/ml when compared to the Control.

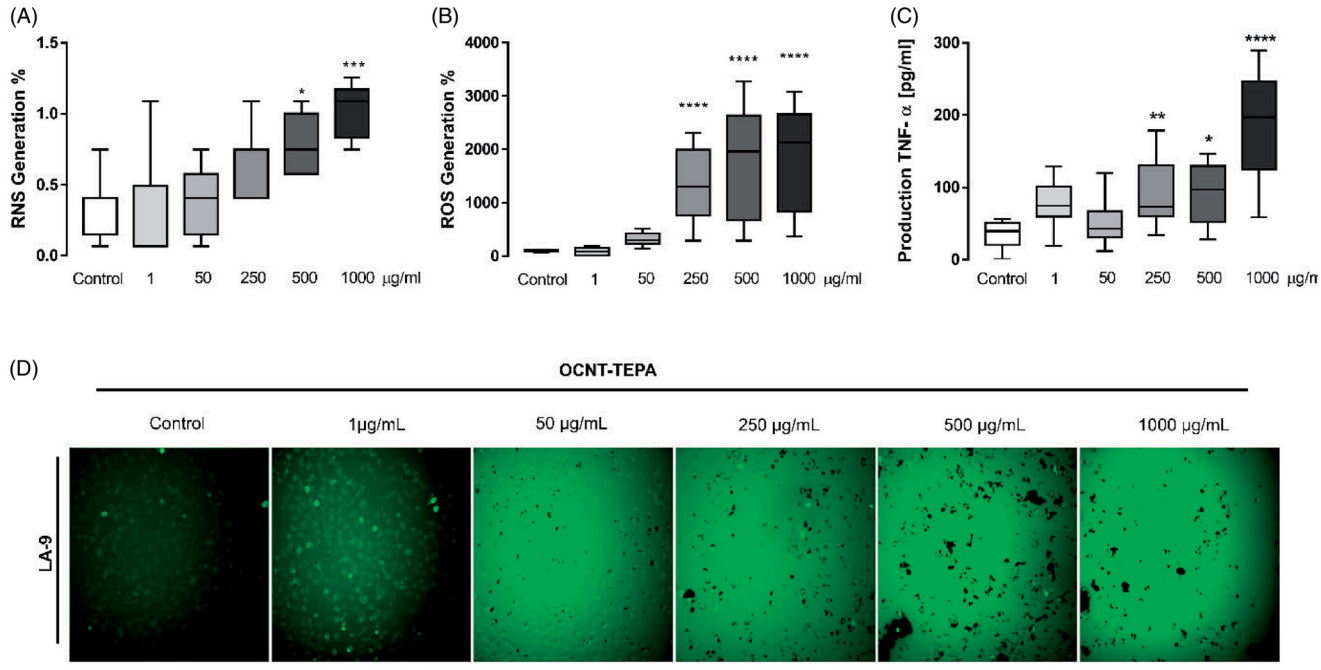


**Figure 8.** Effects of different concentrations of OCNT-TEPA exposure on fibroblasts LA9 related to RNS, ROS and TNF-α production and images intensity of production of ROS after 24 hours of exposure in LA9 cells. Each analyzed concentration (1; 50; 250; 500; and 1000 µg/ml); Control (cells + medium). (a) RNS generation in %; (b) ROS generation in %; (c) Production of TNF-α cytokines; (d) Imagens of intensity of production of ROS. (*) vs. Control; $^{*}p < 0.5$; $^{**}p < 0.01$; $^{***}p > 0.001$; $^{****}p < 0.0001$. The results were presented as the median with the upper and lower quartiles: Me [Q1; Q3].

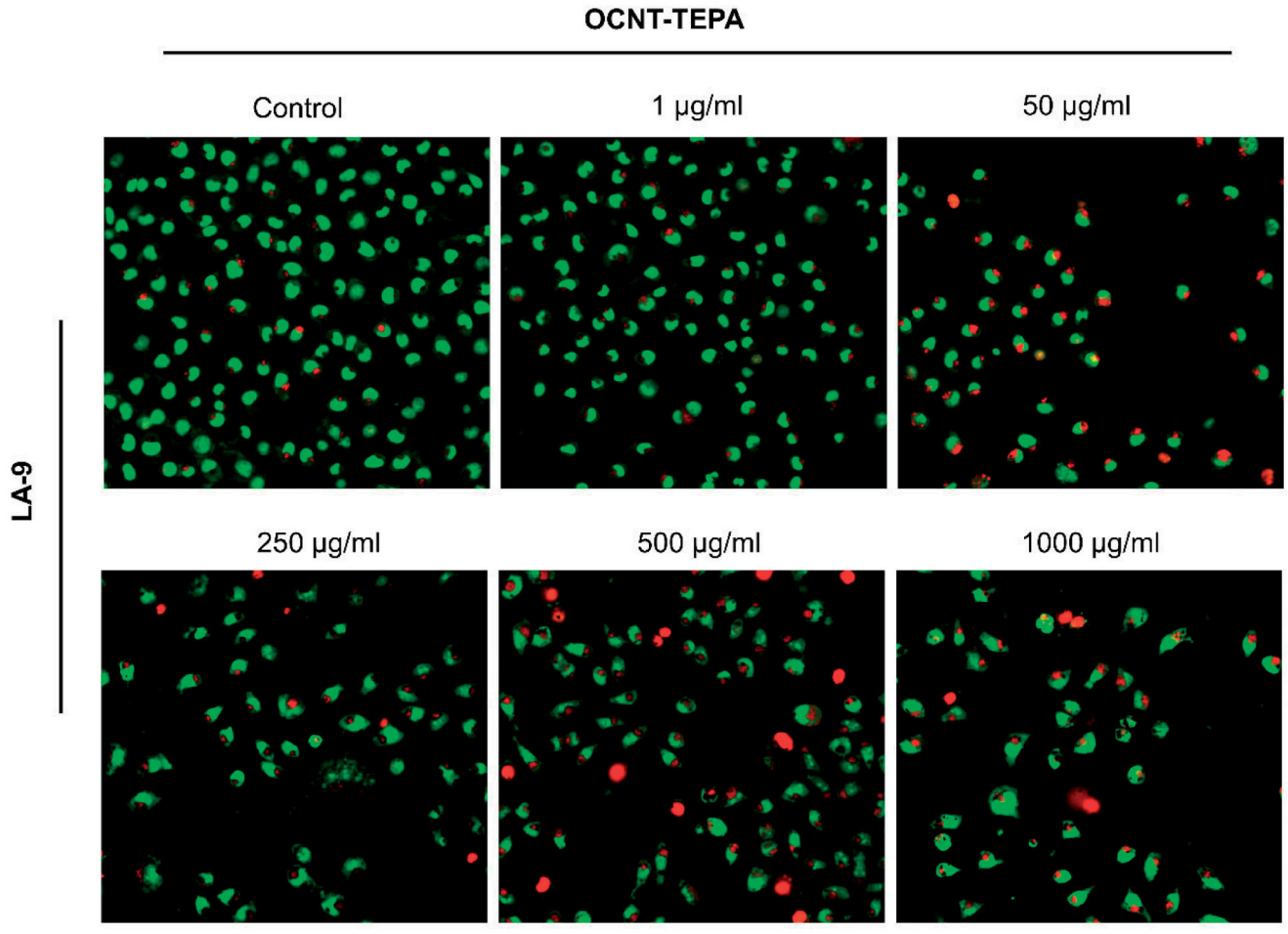


**Figure 9.** Demonstrative analysis of LA 9 fibroblasts stained with LA and IP fluorophores 24 hours after exposure to different concentrations of OCNT-TEPA showing apoptosis/necrosis death through overlapping images obtained using an automated high resolution epifluorescent microscopy system: (a) control, (b) 1 µg/ml, (c) 50 µg/ml, (d) 250 µg/ml, (e) 500 µg/ml, and (f) 1000 µg/ml.

### *Apoptosis – ImageXpress micro*

The Figure 9 shows the high resolution epifluorescent microscopy images made with overlapping from the FITC and TexasRed filters of LA9 cells exposed to different concentrations of OCNT-TEPA for 24 hours and stained with acridine orange, which marks living and dead cells and emits green and with propidium iodide that marks dead cells in which the reddish cytoplasm indicates initial apoptosis and the reddish nucleus indicates late apoptosis and necrosis. A reduction in the number of cells at concentrations of 50, 250, 50, and 1000 μg/ml was observed, in addition to the presence of necrotic cells stained in red.

### *Apoptosis – flow cytometry*

The characterization of the pathway of death (apoptosis/necrosis) of the LA9 fibroblasts was carried out after the cells were exposed to the different concentrations of OCNT-TEPA for 24 hours. The interaction between OCNT-TEPA and the cell death pathway was analyzed by apoptosis (early/late) and necrosis. A panel (qualitative data), containing the proportion of the expression PE Anexina V and 7AAD markers was assembled for all concentrations tested (control, 1, 50, 250,500, and 1000 μg/ml) (Figure 10(a)) and represent the histograms according to each concentration analyzed in 24 hours. The Figure 10(b,c) represents each peak of fluorescence emission from both markers. For apoptosis (Figure 10(c)), it was observed that at concentration of 250 μg/ml there was a significant increase in expression when compared to the control. The Figure 10(e) shows the results for the necrosis analysis, which indicates a significant increase for the 1000 μg/ml OCNT-TEPA concentration compared to the control. The Figure 10(f) represents the correlation between apoptosis and necrosis pathways.

## Discussion

The evaluation of the cytotoxicity of nanomaterials has been carried out, in large part, by cell viability assays, mainly in the acute phase of exposure. These assays can be determined by several pathways such as mitochondrial activity, membrane integrity and cell proliferation (Luanpitpong et al. 2014). Currently, many studies with nanoparticles in biological systems have been reported, since the dispersion of these materials on micro and nanoscale in the environment is inevitable (Azari and Mohammadian 2020).

The new carbon nanotube used in this study, was functionalized by the tetraethylpetamine ligand (TEPA) to improve its physical-chemical characteristics (viscosity, temperature and salinity resistance, stability), making it more interesting for industrial use. However, the consequences that this modification in the nanoparticle can generate, in biological environments, have not been elucidated. The present study was the first to test this functionalized nanotube in a murine fibroblast lineage LA9.

Cellular responses to OCNT-TEPA were assessed by measurements of cell cytotoxicity, oxidative stress, apoptosis and necrosis. In addition, nontoxic doses of the nanoparticle were also investigated in order to assess the safety of the use of these materials. During the characterization of OCNT-TEPA phenomena of change in size, morphology and surface charge change were observed. This can occur due to the interaction of CNTs with the environment, because the reactivity of CNTs is high and there are numerous biomolecules that can interact with them, such as proteins, polysaccharides, peptidoglycans, lipids, humic acid, etc.(Lawrence et al. 2016). In this way, the environment in which CNTs are been used play a fundamental role in observed changes, with the formation of superficial protein corona in CNTs being the main factor for the agglomeration and morphological changes of these nanoparticles (Lynch and Dawson 2008; Cai et al. 2013; Lanone et al. 2013; Zhang et al. 2013)

Analyzes of cell viability of LA9 fibroblasts when exposed to OCNT-TEPA for 24 hours, showed that at concentrations of 250, 500, and 1000 μg/ml there was a change in viability in a dose-dependent manner. This data corroborates the findings by Azari and Mohammadian (2020), who also used the MTT technique to relate the comparison of cell viability of human lung cells A549 after exposure to MWCNTs (Azari and Mohammadian 2020). Studies with human dermal fibroblasts and NIH 3T3 murine fibroblasts also found a significant decrease in cell viability when exposed to 50 e 100 μg/ml of MWCNTs, with human fibroblasts being more sensitive when in contact with MWCNTs (Zhang et al. 2011). In addition, the cytotoxic effects observed by exposure to OCNT-TEPA to MTT assay were also observed during optical microscopy analysis in the morphology assay.

The MTT assay in that study also determined the EC50 value of 115 μg/ml for OCNT-TEPA. Similarly, Ali-Boucetta et al. (2011), observed that the reduction in the viability of fibroblasts cells A549 was 125 μg/ml of MWCNT, being considered very close to what was determined in our study (Ali-Boucetta et al. 2011). In contrast, Zhang et al. (2011), demonstrated in the cell line HeLa after 24 hours of exposure to MWCNTs, different $EC_{50}$ values (341.5, 179.8, and 71.8 μg/ml) for CNTan, CNTir and CNTox (MWCNT with oxidation prepared using deferral methods) (Zhang et al. 2011).

A possible explanation for the different results described above may be related to the functional groups and the surface area of each CNTs, which are able to modify the interaction with the cellular lipid bilayer, which significantly alters the biocompatibility (such as pharmacokinetics and toxicity) of the these nanomaterials (Lopez et al. 2004; Sharma et al. 2019).

Vuković et al. (2009), point out the relationship between cytotoxicity and decreased proliferative activity of fibroblasts L929 when exposed to two different types of MWCNTs, one primary and one functionalized with amino (DETA, TETA, HAD and PDA) (Vuković et al. 2009). In addition, the high concentrations of carbon nanotube generate accumulation of nanoparticles forming clusters, varying the size and making these concentrations more toxic, as seen in the OCNT-TEPA characterization analyzes.

In order to confirm the data from the cell viability, we used the clonogenic assay, which is considered a useful tool

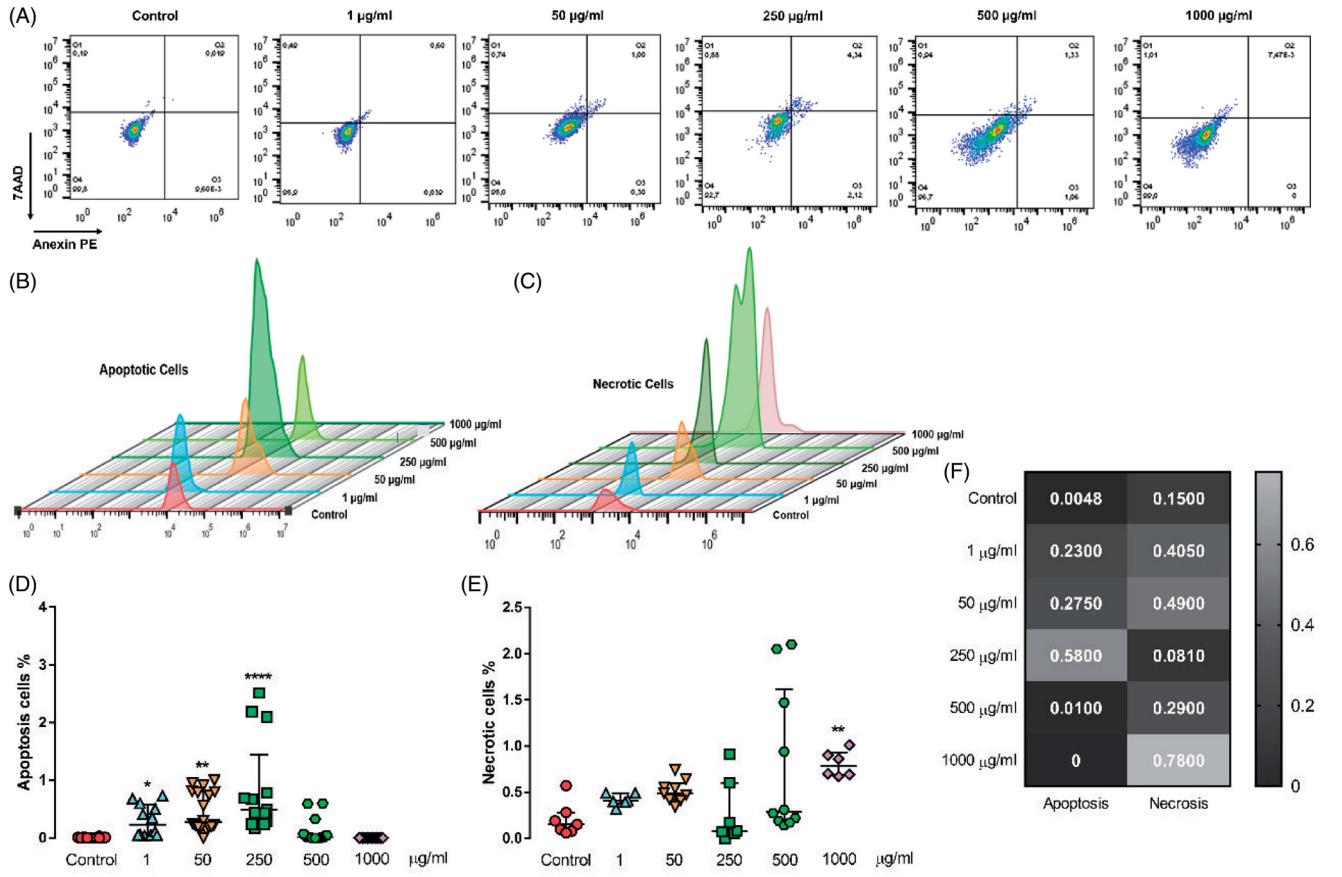


**Figure 10.** Analysis of cell death by apoptosis and necrosis in flow cytometry with the PE Anexin V and 7AAD markers. Each analyzed concentration (1; 50; 250; 500; and 1000 µg/ml) and Control (cells + medium). (a) Histograms of each concentration. (b, c) Each peak of fluorescence emission. (d, e) Percentage of apoptotic and necrotic cells. (f) Represents the correlation between apoptosis and necrosis pathways. (*) vs. Control; *$p < 0.5$; **$p < 0.01$; ***$p > 0.001$; ****$p < 0.0001$. The results were presented as the median with the upper and lower quartiles: Me [Q1; Q3].

in the cytotoxicity of NTCs. Several authors suggest this methodology within nanotoxicology, as long as an appropriate cell line is used (Herzog et al. 2007; Gellein et al. 2009). In this study, the use of the murine fibroblasts LA9 strain was ideal for carrying out the clonogenic assay, since this cell type grows in the form of colonies. The results of our study report the great difficulty of fibroblasts proliferation when exposed to concentrations of OCNT-TEPA for 24 hours. The same effect occurred in the data obtained by Louro et al. (2016), who described that all the MWCNTs tested caused significant decreases in the proliferative capacity of cells A549, 8 days after exposure (Louro et al. 2016).

It is important to highlight that one of the main causes of NTC-induced cytotoxicity is oxidative stress (Shvedova et al. 2012; Liu et al. 2013; Yan et al. 2019). The process of cellular metabolism that occurs in mitochondria naturally generates ROS that are of great importance for cellular homeostasis, and can be easily altered by external environmental stress and consequently produce excessive amounts of ROS that lead to instability of mitochondrial functions (Xie et al. 2016). To confirm the mechanism of mitochondrial dysfunction induced by OCNT-TEPA, the capacity of this CNTto induce oxidative stress by detecting levels of intracellular ROS was evaluated.

The production of ROS occurs when carbon nanotubes are internalized in the cells. At this moment, there is an increase in ROS levels, which can cause cellular damage, such as the destruction of the cell structure, break of the DNA strand and peptide chain and lipid peroxidation, leading to cell death (Dong and Ma 2015; Hiraku et al. 2016; Chestkov et al. 2018; Luceri et al. 2018; Dey et al. 2019; Yan et al. 2019).

As expected, In the present study, an increase in ROS production levels was detected in concentrations above 50 µg/ml of OCNT-TEPA in a dose-dependent manner, as well as in the study by Azari and Mohammadian (2020), who tested different carbon nanotubes in human A549 lung cells and observed an increase in ROS production at all concentrations tested (Azari and Mohammadian 2020). Zhou et al. (2017) also demonstrated the presence of ROS, using human A549 lung cells in contact with 3 different carbon nanotubes that produced ROS at a concentration of 20 µg/ml in the 3 MWCNTs (Zhou et al. 2017).

Along with the ROS, the Reactive Nitrogen Species (RNS) act in the accumulation of damage to the cells, causing nitrosative stress (Singh et al. 2012). The production of nitric oxide (NO) alters the cell's metabolic profile by inhibiting mitochondrial activity via the cytochrome c oxidase pathway

(inhibiting its IV complex) and promoting glycolytic activity, causing cell damage (Almeida et al. 2004; Tauffenberger and Magistretti 2021). Therefore, the measurement of RNS through the production of NO, was carried out in this study to complement the results of ROS since there was production of RNS in the LA9 fibroblasts in the concentrations of 500 and 1000 μg/ml of OCNT-TEPA.

Adding to these pathways, there is also evidence of the involvement of ROS in the extrinsic pathway of apoptosis. This pathway involves death receptors of the tumor necrosis factor (TNF) superfamily (Marchi et al. 2012). In the present study, the measurement of TNF-α was evaluated in LA9 murine fibroblasts and showed a significant increase for concentrations of 250, 500 and 1000 μg/ml of OCNT-TEPA indicating possible inflammatory levels. Research including several types of cells, such as macrophages, bronchial and alveolar epithelia, keratinocytes and fibroblasts, demonstrated that MWCNT stimulated the production of inflammatory mediators, such as TNF-α (He et al. 2011, Schindelin et al. 2012).

In general, there is a correlation between viability data for mitochondrial activity, oxidative stress and TNF-α pathway, in concentrations of 250, 500 and 1000 μg/ml of OCNT-TEPA. Remembering that TNF-α is an apoptosis-mediating cytokine, the cell death pathway was also evaluated in this study by flow cytometry using apoptosis and necrosis markers for LA9 fibroblast cells exposed to OCNT-TEPA for 24 hours. The results showed a high apoptosis index for the concentration of 250 μg/ml of OCNT-TEPA, which decreased in the concentrations of 500 and 1000 μg/ml. On the other hand, the necrosis marker showed low detection at 250 μg/ml and increased necrosis at concentrations of 500 and 1000 μg/ml of OCNT-TEPA. This shows us that there is apoptosis in up to 250 μg/ml of OCNT-TEPA and in the above concentrations (500 and 1000 μg/ml) there is cell death due to necrosis. These data were also observed by Zhou et al. (2017) when they analyzed the exposure of MWCNT in lung A549 cells and observed that in the lowest concentrations there was the presence of apoptosis and in the highest concentrations there was necrotic cell death. The reduction in apoptosis can be explained by the aggregation of MWCNT, because in lower concentrations, where the nanotubes are more dispersed, there is a predominance of cell death due to apoptosis. When the concentration increases, the aggregates in the medium increase and this can alter the mechanism of cell death by rupture of the membrane, causing necrosis of the cells (Zhou et al. 2017). The complementary images of the IMAGE XPRESS equipment (Figure 12F) confirm these data for the LA9 strain.

Considering that the 1000 μg/ml concentration of OCNT-TEPA in this study presented significant data for necrosis of LA9 cells, we can correlate this data with the data obtained by measuring lactate dehydrogenase (LDH), which is an enzyme present in the cytoplasm of cells and is released into the cell culture supernatant when the cell membrane breaks. LDH release characterizes cells in necrosis and was significantly increased at the concentration of 1000 μg/ml from OCNT-TEPA to LA9 (Kumar et al. 2018).

In general, the data presented in this study revealed that OCNT-TEPA altered the viability of LA-9 at concentrations above 50 μg/ml, modifying the mitochondria activity of cells through the overdose of ROS and RSN in these considerations, causing inflammatory activity due to high dosages of TNF-α and promotes cell apoptosis. However, the extent of apoptosis was reduced when the concentration of OCNT-TEPA increased to 1000 μg/ml. This reduction can be explained by the aggregation of nanotubes, which altered the mechanism of cell death from apoptosis to rupture of the membrane, generating necrosis.

## Conclusion

The results obtained in the study of the OCNT-TEPA carbon nanoparticle to determine its biological effect through well-established cytotoxicity tests on LA9 murine fibroblasts, show that the analyzed carbon nanotube showed cytotoxic potential, being dependent on concentration. In general, there was a reduction in cell viability, damage to the cell membrane, a decrease in proliferative capacity, an increase in reactive oxygen and nitrogen species and an inflammatory profile for a 24-hour exposure period. These analyzes are extremely important, as this nanoparticle was synthesized for use in industry, which makes it able to circulate in the environment and in contact with organisms, can cause irreparable damage.

## Acknowledgments

The authors would like to thank Professor Márcia Regina Cominetti (Department of Gerontology, Federal University of São Carlos – UFSCar) for the availability of equipment, to Lilian Tan Moriyama (Laboratory of Biophotonics of the Research Center in Optics and Photonics – CEPOF-of the São Carlos Institute of Physics, University of São Paulo), for her assistance in the analysis of spectroscopy and Camila Tita Nogueira, Ph.D, for their valuable contributions.

## Disclosure statement

No potential conflict of interest was reported by the author(s).

## Funding

This work was supported by PETROBRAS/Project: Proc. No 2017/00010-7.

## References

Ali-Boucetta H, et al. 2011. Cellular uptake and cytotoxic impact of chemically functionalized and polymer-coated carbon nanotubes. Small. 7(22):3230–3238.

Almeida A, Moncada S, Bolaños JP. 2004. Nitric oxide switches on glycolysis through the AMP protein kinase and 6-phosphofructo-2-kinase pathway. Nat Cell Biol. 6(1):45–51.

Aqel A, El-Nour KMMA, Ammar RAA, Al-Warthan A. 2012. Carbon nanotubes, science and technology part (I) structure, synthesis and characterisation. Arabian J Chem. 5(1):1–23.

Aschberger K, Johnston HJ, Stone V, Aitken RJ, Hankin SM, Peters SAK, Tran CL, Christensen FM. 2010. Review of carbon nanotubes toxicity

and exposure-appraisal of human health risk assessment based on open literature. Crit Rev Toxicol. 40(9):759–790.
Azari RM, Mohammadian Y. 2020. Comparing in vitro cytotoxicity of graphite, short multi-walled carbon nanotubes, and long multi-walled carbon nanotubes. Environ Sci Pollut Res. 27(13):15401–15406.
Beer C, Foldbjerg R, Hayashi Y, Sutherland DS, Autrup H. 2012. Toxicity of silver nanoparticles-nanoparticle or silver ion? Toxicol Lett. 208(3):286–292.
Bicho RC, Roelofs D, Mariën J, Scott-Fordsmand JJ, Amorim MJB. 2020. Epigenetic effects of (nano)materials in environmental species – Cu case study in *Enchytraeus crypticus*. Environ Int. 136(December 2019): 105447.
Binelli A, Magni S, La Porta C, Bini L, Della Torre C, Ascagni M, Maggioni D, Ghilardi A, Armini A, Landi C, et al. 2018. Cellular pathways affected by carbon nanopowder-benzo(α)pyrene complex in human skin fibroblasts identified by proteomics. Ecotoxicology and Environmental Safety. 160(May):144–153.
Cai X, Ramalingam R, Wong HS, Cheng J, Ajuh P, Cheng SH, Lam et YW. 2013. Characterization of carbon nanotube protein corona by using quantitative proteomics. Nanomedicine: Nanotechnology, Biology and Medicine. Elsevier B.V.
Chestkov IV, Jestkova EM, Ershova ES, Golimbet VG, Lezheiko TV, Kolesina NY, Dolgikh OA, Izhevskaya VL, Kostyuk G, Kutsev SI, et al. 2018. ROS-induced DNA damage associates with abundance of mitochondrial DNA in white blood cells of the untreated schizophrenic patients. Oxid Med Cell Longevity. 2018:1–7.
Clichici S, Biris AR, Tabaran F, Filip A . 2012. Transient oxidative stress and inflammation after intraperitoneal administration of multiwalled carbon nanotubes functionalized with single strand DNA in rats. Toxicol Appl Pharmacol. 259(3):281–292.
Dey U, Ghosh A, Abbas S, Taraphder A, Roy M. 2019. Cell damage and mitigation in Swiss albino mice: experiment and modelling. Alexandria Engineering Journal. 59:1345–1357.
DE Volder MFL, Tawfick SH, Baughman RH, Hart AJ. 2013. Carbon nanotubes: present and future commercial applications. Science. 339(6119):535–539.
Dl Cristo L, Bianchi MG, Taurino G, Donato F, Garzaro G, Bussolati O, Bergamaschi E. 2019. Comparative in vitro cytotoxicity of realistic doses of benchmark Multi-Walled Carbon Nanotubes towards macrophages and airway epithelial cells. Nanomaterials. 9(7):98.
Dong J, Ma Q. 2015. Advances in mechanisms and signaling pathways of carbon nanotube toxicity. Nanotoxicology. 9(5):658–676.
Du J, Ge C, Liu Y, Bai R, Li D, Yang Y, Liao L, Chen C. 2011. The interaction of serum proteins with carbon nanotubes depend on the physicochemical properties of nanotubes. J Nanosci Nanotechnol. 11(11): 10102–10110.
Endo M. 1988. Grow carbon fibers in the vapor phase. Chem Tech. 568–576.
Firme CP, Bandaru PR. 2010. Toxicity issues in the application of carbon nanotubes to biological systems. Nanomed Nanotechnol Biol Med. 6(2):245–256.
Franken NAP, et al. 2006. Clonogenic assay of cells *in vitro*. Nat Protoc. 1(5):2315–2319.
Gellein K, Hoel S, Gellein K, Hoel S, Evje L, Syversen T. 2009. The colony formation assay as an indicator of carbon nanotube toxicity examined in three cell lines. Nanotoxicology. 3(3):215–221.
Georgakilas V, Perman JA, Tucek J, Zboril R. 2015. Broad family of carbon nanoallotropes: classification, chemistry, and applications of fullerenes, carbon dots, nanotubes, graphene, nanodiamonds, and combined superstructures. Chem Rev. 115(11):4744–4822.
Green LC, Wagner DA, Glogowski J, Skipper PL, Wishnok JS, Tannenbaum SR. 1982. Analysis of nitrate, nitrite, and [15N]nitrate in biological fluids. Anal Biochem. 126(1):131–138.
He X, Shih-Houng Y, Fernback JE, Ma Q. 2012. Single-walled carbon nanotubes induce fibrogenic effect by disturbing mitochondrial oxidative stress and activating NF-jB signaling. J Clin Toxicol. s5(01):2–8.
He X, Young SH, Schwegler-Berry D, Chisholm WP, Fernback JE, Ma Q. 2011. Multiwalled carbon nanotubes induce a fibrogenic response by stimulating reactive oxygen species production, activating NF-jB signaling, and promoting fibroblast-to-myofibroblast trans formation. Chem Res Toxicol. 24(12):2237–2248.
Herzog E, Casey A, Lyng FM, Chambers G, Byrne HJ, Davoren M. 2007. A new approach to the toxicity testing of carbonbased nanomaterials-The clonogenic assay. Toxicol Lett. 174(1–3):49–60.
Hiraku Y, Guo F, Ma N, Yamada T, Wang S, Kawanishi S, Murata M. 2016. Multi-walled carbon nanotube induces nitrative DNA damage in human lung epithelial cells via HMGB1-RAGE interaction and Toll-like receptor 9 activation. Part Fibre Toxicol. 13(1):1–21.
Holsapple MP, Farland WH, Landry TD, Monteiro-Riviere NA, Carter JM, Walker NJ, Thomas KV. 2005. Research strategies for safety evaluation of nanomaterials, part II: toxicological and safety evaluation of nanomaterials, current challenges and data needs. Toxicol Sci. 88(1):12–17.
Hurt RH, Monthioux M, Kane A. 2006. Toxicology of carbon nanomaterials: status, trends, and perspectives on the special issue. Carbon. 44(6):1028–1033.
Iijima S. 1991. Helical microtubules of graphitic carbon. Vol. 354. Nature Publishing Group; p. 56–58.
Jain S, Singh SR, Pillai S. 2012. Toxicity issues related to biomedical applications of carbon nanotubes. J Nanomed Nanotechnol. 3(5):2–15.
Jeevanandam J, Barhoum A, Chan YS, Dufresne A, Danquah MK. 2018. Review on nanoparticles and nanostructured materials: history, sources, toxicity and regulations. Beilstein J Nanotechnol. 9(1):1050–1074.
Khan I, Saeed K, Khan I. 2019. Nanoparticles: properties, applications and toxicities. Arabian J Chem. 12(7):908–931.
Kobayashi N, Izumi H, Morimoto Y. 2017. Review of toxicity studies of carbon nanotubes. J Occup Health. 59(5):394–407.
Kumar P, Nagarajan A, Uchil PD. 2018. Analysis of cell viability by the lactate dehydrogenase assay. Cold Spring Harbor Protocols. 2018(6): 465–468.
Lanone S, Lanone S, Andujar P, Kermanizadeh A, Boczkowski J. 2013. Determinants of carbon nanotube toxicity. Adv Drug Delivery Rev. 65(15):2063–2069.
Lawrence JR, Swerhone GDW, Dynes JJ, Hitchcock AP, Korber DR. 2016. Complex organic corona formation on carbon nanotubes reduces microbial toxicity by suppressing reactive oxygen species production. Environ Sci: Nano. 3(1):181–189.
Lima MCFS, Amparo S. Z S d, Siqueira EJ, Miquita DR, Caliman V, Silva GG. 2018. Polyacrylamide copolymer/aminated carbon nanotube-based aqueous nanofluids for application in high temperature and salinity. J Appl Polym Sci. 135(25):46382–46310.
Liu Y, Zhao Y, Sun B, Chen C. 2013. Understanding the toxicity of carbon nanotubes. Acc Chem Res. 46(3):702–713.
Lopez CF, Nielsen SO, Moore PB, Klein ML. 2004. Understanding nature's design for a nanosyringe. PNAS. 101(13):4431–4434.
Louro H, Pinhão M, Santos J, Tavares A, Vital N, Silva MJ. 2016. Evaluation of the cytotoxic and genotoxic effects of benchmark multiwalled carbon nanotubes in relation to their physicochemical properties. Toxicol Lett. 262:123–134.
Luanpitpong S, Wang L, Rojanasakul Y. 2014. The effects of carbon nanotubes on lung and dermal cellular behaviors. Nanomedicine. 9(6): 895–912.
Luceri C, Bigagli E, Femia AP, Caderni G, Giovannelli L, Lodovici M. 2018. Aging related changes in circulating reactive oxygen species (ROS) and protein carbonyls are indicative of liver oxidative injury. Toxicol Rep. 5(November 2017):141–145.
Lynch I, Dawson KA. 2008. Protein-nanoparticle interactions. Nanotoday. 3:40–47.
Mannerström M, Zou J, Toimela T, Pyykkö I, Heinonen T. 2016. The applicability of conventional cytotoxicity assays to predict safety/toxicity of mesoporous silica nanoparticles, silver and gold nanoparticles and multi-walled carbon nanotubes. Toxicol in Vitro. 37:113–120.
Marchi S, Giorgi C, Suski JM, Agnoletto C, Bononi A, Bonora M, De Marchi E, Missiroli S, Patergnani S, Poletti F, et al. 2012. Mitochondria-Ros crosstalk in the control of cell death and aging. J Signal Transduct. 2012:1–17.
Mohanta D, Patnaik S, Sood S, Das N. 2019. Carbon nanotubes: evaluation of toxicity at biointerfaces. J Pharm Anal. 9(5):293–300.

Mosmann T. 1983. Rapid colorimetric assay for cellular growth and survival: application to proliferation and cytotoxicity assays. J Immunol Methods. 65(1–2):55–63.

Nel A, Xia T, Mädler L, Li N. 2006. Toxic potential of materials at the nanolevel. Science. 311(5761):622–627.

Patil SS, Lekhak UM. 2020. Toxic effects of engineered carbon nanoparticles on environment. Micro and Nano Technologies. Elsevier Inc.; p. 237–260.

Pikula K, Chaika V, Zakharenko A, Markina Z, Vedyagin A, Kuznetsov V, Gusev A, Park S, Golokhvast K. 2020. Comparison of the level and mechanisms of toxicity of carbon nanotubes, carbon nanofibers, and silicon nanotubes in bioassay with four marine microalgae. Nanomaterials. 10(3):485.

Pikula K, Zakharenko A, Chaika V, Kirichenko K, Tsatsakis A, Golokhvast K. 2020. Risk assessments in nanotoxicology: bioinformatics and computational approaches. Curr Opin Toxicol. 19:1–6.

Prajapati SK, Malaiya A, Kesharwani P, Soni D, Jain A. 2020. Biomedical applications and toxicities of carbon nanotubes. Drug Chem Toxicol. 1–16.

Saltzman BE. 1954. Colorimetric microdetermination of nitrogen dioxide in the atmosphere. Anal Chem. 26(12):1949–1955.

Savolainen K, Alenius H, Norppa H, Pylkkänen L, Tuomi T, Kasper G. 2010. Risk assessment of engineered nanomaterials and nanotechnologies-a review. Toxicology. 269(2–3):92–104.

Schindelin J, Arganda-Carreras I, Frise E, Kaynig V. 2012. Fiji: an open-source platform for biological image analysis. Nat Methods. 9(7):676–682.

Sharma S, Naskar S, Kuotsu K. 2019. A review on carbon nanotubes: Influencing toxicity and emerging carrier for platinum based cytotoxic drug application. J Drug Delivery Sci Technol. 51(March):708–720.

Shetty AM, Wilkins GMH, Nanda J, Solomon MJ. 2009. Multiangle depolarized dynamic light scattering of short functionalized single-walled carbon nanotubes. J Phys Chem C. 113(17):7129–7133.

Shvedova AA, Pietroiusti A, Fadeel B, Kagan VE. 2012. Mechanisms of carbon nanotube-induced toxicity: Focus on oxidative stress. Toxicol Appl Pharmacol. 261(2):121–133.

Singh RP, Manasmita Das, Thakare V, Jain S. 2012. Erratum: Functionalization density dependent toxicity of oxidized multiwalled carbon nanotubes in a murine macrophage cell line. Chem Res Toxicol. 25(11):2617.

Tauffenberger A, Magistretti PJ. 2021. Reactive oxygen species: beyond their reactive behavior. Neurochem Res. 46(1):77–87.

Torresan M, Wolosiuk A. 2021. Critical aspects on the chemical stability of NaYF4-based upconverting nanoparticles for biomedical applications. ACS Appl. Bio Mater. 4(2):1191–1210.

Veloz-Castillo MF, Paredes-Arroyo A, Vallejo-Espinosa G, Delgado-Jiménez JF, Coffer JL, González-Rodríguez R, Mendoza ME, Campos-Delgado J, Méndez-Rojas MA. 2020. Carbon nanotubes and carbon fibers in a flash: an easy and convenient preparation of carbon nanostructures using a conventional microwave. Can J Chem. 98(1):49–55.

Vuković G, Marinković A, Obradović M, Radmilović V, Čolić M, Aleksić R, Uskoković PS. 2009. Synthesis, characterization and cytotoxicity of surface amino-functionalized water-dispersible multi-walled carbon nanotubes. Appl Surf Sci. 255(18):8067–8075.

Wan CP, Myung E, Lau BHS. 1993. An automated micro-fluorometric assay for monitoring oxidative burst activity of phagocytes. J Immunol Meth. 159(1–2):131–138.

Xie Y, Liu D, Cai C, Chen X, Zhou Y, Wu L, Sun Y, Dai H, Kong X, Xie Y. 2016. Size-dependent cytotoxicity of Fe3O4 nanoparticles induced by biphasic regulation of oxidative stress in different human hepatoma cells. IJN. 11:3557–3570.

Yan H, Xue Z, Xie J, Dong Y, Ma Z, Sun X, Kebebe Borga D, Liu Z, Li J. 2019. Toxicity of carbon nanotubes as anti-tumor drug carriers. IJN. 14:10179–10194.

Yang M-c, Li M-y, Luo S, Liang R. 2016. Real-time monitoring of carbon nanotube dispersion using dynamic light scattering and UV-vis spectroscopy. Int J Adv Manuf Technol. 82(1-4):361–367.

Yoksan R, Chirachanchai S. 2008. Amphiphilic chitosan nanosphere: studies on formation, toxicity, and guest molecule incorporation. Bioorg Med Chem. 16(5):2687–2696.

Yuan X. 2019. Cellular toxicity and immunological effects of carbonbased nanomaterials. Part Fibre Toxicol. 16(1):2–27.

Zhang J, Landry MP, Barone PW, Kim JH. 2013. Molecular recognition using corona phase complexes made of synthetic polymers adsorbed on carbon nanotubes. Nat Nanotechnol. 8(12):959–968.

Zhang Y, Wang B, Meng X, Sun G, Gao C. 2011. Influences of acid-treated multiwalled carbon nanotubes on fibroblasts: Proliferation, adhesion, migration, and wound healing. Ann Biomed Eng. 39(1):414–426.

Zhao S, Su X, Wang Y, Yang X, Bi M, He Q, Chen Y. 2020. Copper oxide nanoparticles inhibited denitrifying enzymes and electron transport system activities to influence soil denitrification and N2O emission. Chemosphere. 245:125394.

Zhou L, Forman HJ, Ge Y, Lunec J. 2017. Multi-walled carbon nanotubes: a cytotoxicity study in relation to functionalization, dose and dispersion. Toxicol in Vitro. 42:292–298.